

Published in final edited form as:

J Comp Neurol. 2014 September 1; 522(13): 3120–3137. doi:10.1002/cne.23582.

Compromised Blood-Brain Barrier Competence in Remote Brain Areas in Ischemic Stroke Rats at Chronic Stage

Svitlana Garbuzova-Davis^{1,2,3,4,*}, Edward Haller⁵, Stephanie N. Williams¹, Eithan D. Haim¹, Naoki Tajiri¹, Diana G. Hernandez-Ontiveros¹, Aric Frisina-Deyo¹, Sean M. Boffeli¹, Paul R. Sanberg^{1,2,4,6}, and Cesario V. Borlongan^{1,2}

¹Center of Excellence for Aging & Brain Repair, University of South Florida, Morsani College of Medicine, Tampa, Florida 33612, United States of America

²Department of Neurosurgery and Brain Repair, University of South Florida, Morsani College of Medicine, Tampa, Florida 33612, United States of America

³Department of Molecular Pharmacology and Physiology, University of South Florida, Morsani College of Medicine, Tampa, Florida 33612, United States of America

⁴Department of Pathology and Cell Biology, University of South Florida, Morsani College of Medicine, Tampa, Florida 33612, United States of America

⁵Department of Integrative Biology, University of South Florida, Tampa, Florida 33620, United States of America

⁶Department of Psychiatry, University of South Florida, Morsani College of Medicine, Tampa, Florida 33612, United States of America

Abstract

Stroke is a life threatening disease leading to long-term disability in stroke survivors. Cerebral functional insufficiency in chronic stroke might be due to pathological changes in brain areas remote from initial ischemic lesion, i.e. diaschisis. Previously, we showed that the damaged blood-brain barrier (BBB) was implicated in subacute diaschisis. The present study investigated BBB competence in chronic diaschisis using a transient middle cerebral artery occlusion (tMCAO) rat model. Our results demonstrated significant BBB damage mostly in the ipsilateral striatum and motor cortex in rats at 30 days after tMCAO. The BBB alterations were also determined in the contralateral hemisphere via ultrastructural and immunohistochemical analyses. Major BBB pathological changes in contralateral remote striatum and motor cortex areas included: (1) vacuolated endothelial cells containing large autophagosomes, (2) degenerated pericytes displaying mitochondria with cristae disruption, (3) degenerated astrocytes and perivascular

* Author for correspondence: Svitlana Garbuzova-Davis, Ph.D., D.Sc., Center of Excellence for Aging and Brain Repair, Department of Neurosurgery and Brain Repair, University of South Florida, Morsani College of Medicine, 12901 Bruce B. Downs Blvd., Tampa, FL 33612, Tel: 813-974-3189, Fax: 813-974-3078, sgarbuza@health.usf.edu.

Conflict of Interest Statement: The authors declare no conflict of interest.

All authors had full access to all the data in the study and take responsibility for the integrity of the data and the accuracy of the data analysis. Study concept and design: SGD, PRS, CVB. Electron microscopy: EH. Acquisition of data: NT, DGHO, AFD, SNW, EDH. Analysis and interpretation of data: SGD, EH, SNW, EDH, SMB. Drafting of the manuscript: SGD. Critical revision of the manuscript for important intellectual content: EH, PRS, CVB. Statistical analysis: CVB. Surgery: CVB. Technical support: EH. Study supervision: SGD, CVB.

edema, (4) Evans Blue extravasation, and (5) appearance of parenchymal astrogliosis. Importantly, discrete analyses of striatal and motor cortex areas revealed significantly higher autophagosome accumulation in capillaries of ventral striatum and astrogliosis in dorsal striatum in both cerebral hemispheres. These widespread microvascular alterations in ipsilateral and contralateral brain hemispheres suggest persistent and/or continued BBB damage in chronic ischemia. The pathological changes in remote brain areas likely indicate chronic ischemic diaschisis, which should be considered in the development of treatment strategies for stroke.

Keywords

MCAO; rats; BBB; chronic diaschisis; autophagosomes; astrocytes

INTRODUCTION

Stroke is a serious life threatening disease and the fourth leading cause of death in the USA (Anon, 2012). On average, every 40 seconds someone has a stroke and every 4 minutes someone dies of a stroke (Anon, 2012; Go et al., 2013). Due to interruption of blood flow to the brain, stroke is typed as ischemic, intracerebral hemorrhagic, or subarachnoid hemorrhagic. Approximately 87% of strokes are ischemic (Go et al., 2013). Stroke survivors may not fully recover and risk long-term disability (Centers for Disease Control and Prevention (CDC), 2009). Of ischemic stroke survivors at 65 years of age and older, observed at 6 months after stroke, 50% had hemiparesis, 46% had cognitive deficits, and about 30% were dependent in daily living activities (Kelly-Hayes et al., 2003).

The pathologic processes caused by stroke vascular injury occur in a time-dependent manner and are separated into acute (minutes to hours), subacute (hours to days), and chronic (days to months). The cascade of cerebral pathological events arising shortly after initial ischemic stroke insult (reviewed in (Dirnagl et al., 1999; Bramlett and Dietrich, 2004; VanGilder et al., 2012)) might contribute to prolonged and widespread brain damage. Although the size of the primary stroke lesion is important, the location of this lesion is also essential for predicting patient outcome, especially at chronic stage. It has been shown that motor recovery and functional outcome in hemiplegic stroke patients at 1 and 6 months after stroke correlate more strongly with brain lesion size and primary location rather than only with lesion size (Chen et al., 2000). However, post-stroke recovery might also depend on functional changes in remote brain structures, i.e. diaschisis, which are distant from the initial (focal) ischemic lesion. Changes in blood flow and metabolism have been determined in the hemisphere contralateral to unilateral cerebral ischemia, a condition known as transhemispheric diaschisis (Dobkin et al., 1989; Andrews, 1991). Stroke patients who recovered from severe hemiparesis after about 6 months demonstrated overlap between the lesion-affected and recovery-related networks in the contra-lesional thalamus and extrastriate occipital cortex (Seitz et al., 1999). Also, it has been shown that crossed cerebellar diaschisis is associated with infarct hypoperfusion volume in both acute and outcome stages in patients within 72 hours and 3 months of stroke onset, respectively, and “persists despite neurological recovery” (Infeld et al., 1995). In a rat middle cerebral artery occlusion (MCAO) model of transient ischemia, transcortical diaschisis was determined in

the neocortex (Reinecke et al., 1999; Neumann-Haefelin and Witte, 2000), suggesting widespread degeneration of corticostriatal connections. Another study on a focal cortical rat stroke model demonstrated ipsilateral diaschisis in connected cortical regions, which were distant from initial damage (Carmichael et al., 2004).

Amid this complexity of post-ischemic pathological changes, blood-brain barrier (BBB) competence might be critical. Numerous comprehensive studies have identified BBB disruption after stroke (del Zoppo and Hallenbeck, 2000; Brown and Davis, 2002; del Zoppo and Mabuchi, 2003; Persidsky et al., 2006; Sandoval and Witt, 2008; Jin et al., 2010; Lakhan et al., 2013). Increased BBB permeability has been shown in both acute ischemic stroke patients (Dankbaar et al., 2011) and in a rodent model of MCAO (Preston et al., 1993; Yang and Betz, 1994; Belayev et al., 1996; Kahles et al., 2007). Although biphasic (“open-close-open”) BBB leakage separated by a refractory period in ischemic-reperfusion injury was noted between 3 and 24 hours post-MCAO (Kuroiwa et al., 1985; Preston et al., 1993; Belayev et al., 1996; Rosenberg et al., 1998), some studies showed BBB openings lasting up to 4–5 weeks (Strbian et al., 2008; Abo-Ramadan et al., 2009) and possibly aggravating post-ischemic brain injury.

However, despite intensive research into the implications of BBB openings in ischemic stroke, the bulk of these studies have focused on the acute post-stroke stage and the cerebral hemisphere of initial ischemic insult. Recently, we demonstrated BBB alterations not only in the ipsilateral hemisphere, but also in contralateral brain areas, 7 days after transient MCAO in rats, indicating the existence of subacute ischemic diaschisis (Garbuzova-Davis et al., 2013). Mainly, damaged endothelial cells containing numerous autophagosomes, pericyte degeneration, and perivascular edema in addition to vascular leakage, widespread astrogliosis, activated microglia, neuronal pyknosis, and decreased myelin were determined in contralateral striatum, and motor and somatosensory cortices. Since our data revealed microvascular damage is associated with BBB breakdown in brain areas remote from initial ischemic lesion at subacute ischemic stage, an important next step was to investigate BBB competence and diaschisis in chronic ischemic stroke.

The aim of this study was to evaluate chronic diaschisis in a rat model of focal cerebral ischemia. A specific focus was analyzing BBB status in the contralateral cerebral hemisphere, an area with remote brain structures not directly affected by ischemia.

MATERIALS AND METHODS

Ethics Statement

All described procedures were approved by the Institutional Animal Care and Use Committee at USF and conducted in compliance with the *Guide for the Care and Use of Laboratory Animals*.

Animals

All animals used in the study were obtained from The Jackson Laboratory, Bar Harbor, Maine. Thirty two Sprague Dawley adult male rats weighting 260.5 ± 3.15 g were randomly assigned to one of two groups: MCAO (n=15) or control (n=17). All rats were housed in a

temperature-controlled room (23°C) and maintained on a 12:12 h dark: light cycle (lights on at 06:00 AM). Food and water were available ad libitum.

Middle Cerebral Artery Occlusion

Stroke surgery was performed via transient middle cerebral artery occlusion (tMCAO) using the intraluminal filament technique previously described in detail (Borlongan et al., 2004 a; Tajiri et al., 2012; Garbuzova-Davis et al., 2013) and based on our prior standardization of this stroke model (Matsukawa et al., 2009; Yasuhara et al., 2009; Borlongan et al., 2010) showing at least 80% reduction in regional cerebral blood flow in stroke animals during the occlusion period as determined by laser Doppler (Perimed). Briefly, the tip of the filament was customized using a dental cement (GC Corporation, Tokyo, Japan). Body temperature was maintained at $37 \pm 0.3^\circ\text{C}$ during the surgical procedures. The midline skin incision was made in the neck with subsequent exploration of the right common carotid artery (CCA), the external carotid artery, and internal carotid artery. A 4-0 monofilament nylon suture (27.0–28.0 mm) was advanced from the CCA bifurcation until it blocked the origin of the middle cerebral artery (MCA). Animals were allowed to recover from anesthesia during MCAO. At 60 minutes after MCAO, animals were re-anesthetized with 1–2% isoflurane in nitrous oxide/oxygen (69%/30%) using a face mask and reperfused by withdrawal of the nylon thread. A midline incision was made in the neck and the right CCA was isolated. The animals were then closed and allowed to recover from anesthesia.

Perfusion and Tissue Preparation

Thirty days after reperfusion, tMCAO rats and controls were sacrificed under CO₂ inhalation and perfused transcardially with 0.1 M phosphate buffer (PB, pH 7.2) followed by 4% paraformaldehyde (PFA) in phosphate buffer solution under pressure control fluid delivery at 85 mm Hg. tMCAO rats (n=12) and controls (n=15) were intravenously injected with 1 ml of 2% Evans Blue dye (EB, Aldrich Chemical) in saline solution via the jugular vein 30 min prior to perfusion as previously described (Garbuzova-Davis et al., 2013). The surgical procedure was performed in tMCAO and control rats using the same protocol including exposure to anesthesia. Prior to perfusion, blood samples (about 3 ml) were taken through cardiac puncture from randomly selected tMCAO and control rats (n=5/each group) and collected into serum separation tube (Corvac™) for 10 minutes at room temperature (RT). Sera were obtained after centrifugation at 1200 rpm for 15 minutes. Rats assayed for Evans Blue extravasation received only phosphate buffer solution. After perfusion, rat brains were rapidly removed from tMCAO rats (n=9) and controls (n=11) for Evans Blue extravasation assay as described below. Remaining rats receiving an Evans Blue injection were perfused and their brains were immediately removed, fixed intact in 4% paraformaldehyde in 0.1 M phosphate buffer for 24–48 hrs and then cryoprotected in 20% sucrose in 0.1 M phosphate buffer overnight. Coronal brain tissues were cut at 30 μm in a cryostat, thaw-mounted onto slides, and stored at –20°C for immunohistochemical analysis. Rats assayed for electron microscope analysis were randomly chosen from each group (tMCAO, n=3; control, n=2). Rat brains were immediately removed and fixed in 4% paraformaldehyde in 0.1 M phosphate buffer for 16–24 hours at 4°C. The next day, brains were cut into 1 mm slices, mapped against a diagram of the whole slice at Bregma level of 0.20–0.48 mm accordingly to a rat brain atlas (Paxinos and Watson, 1998), and the motor

cortex (M2/M1) and striatum (CPu) regions removed and coded from the slices of both brain hemispheres. Coordinates for ipsi- M1/M2 motor cortex area were about 4 mm ventral and 1.5 mm lateral from the striatum on the coronal section. Coordinates applied for removal of striatum and motor cortex tissues from the contralateral hemisphere were as previously described (Garbuzova-Davis et al., 2013). Tissues were then fixed overnight in 2.5% glutaraldehyde in 0.1M phosphate buffer (Electron Microscopy Sciences, Inc., Hatfield, PA) at 4°C and stored for further electron microscope processing.

BBB Permeability

Evans Blue dye, 961 Da, was used as a tracer for assessing BBB disruption. The Evans Blue extravasation assay was performed as previously described (Borlongan et al., 2004b; Garbuzova-Davis et al., 2013). Briefly, after perfusion, rat brains were divided into right and left hemispheres. Brain tissues were weighed and placed in 50% trichloroacetic acid solution (Sigma). Following homogenization and centrifugation, the supernatant was diluted with ethanol (1:3) and loaded into a 96 well-plate in triplicates. Sera were diluted with ethanol (1:10,000) and loaded separately into a 96 well-plate in triplicates also. The dye was measured with a spectrofluorometer (Gemini EM Microplate Spectrofluorometer, Molecular Devices) at excitation of 620nm and emission of 680nm (Ay et al., 2008). Calculations were based on external standards in the same solvent. The tissue Evans Blue content was quantified from a linear standard curve derived from known amounts of the dye and was normalized to tissue weight ($\mu\text{g/g}$). For sera, Evans Blue concentration was quantified similarly and presented as $\mu\text{g/ml}$. All measurements were performed by two experimenters blinded to the experiment.

Electron Microscopy

Since the cortex and striatum are the areas most affected by MCAO (Nagasawa and Kogure, 1989; Popp et al., 2009) and compromised BBB integrity was determined in remote contralateral brain areas in tMCAO rats at subacute stage (Garbuzova-Davis et al., 2013), structural analysis of microvessels was performed in the motor cortex (M2/M1) and striatum (CPu) of both brain hemispheres in rats 30 days after tMCAO using electron microscopy. Briefly, tissue samples were post-fixed in 1% osmium tetroxide (Electron Microscopy Sciences, Inc., Hatfield, PA) in 0.1M phosphate buffer for 1 hour at room temperature and then dehydrated in a graded series of acetone dilutions. Tissues were transferred to a 50:50 mix of acetone and LX112 epoxy resin embedding mix (Ladd Research Industries, Burlington VT) and infiltrated with this mix for 1 hour. The tissues were then transferred to a 100% LX112 embedding mix and infiltrated with fresh changes of the embedding mix. The tissues were further infiltrated overnight in fresh embedding medium at 4°C. On the following day, the tissues were embedded in a fresh change of resin in tissue capsules. The blocks were polymerized at 70°C in an oven overnight. The blocks were trimmed and then sectioned with a diamond knife on an LKB Huxley ultramicrotome. Thick sections cut at 0.35 μm were placed on glass slides and stained with 1% toluidine blue stain. Thin sections were cut at 80–90nm, placed on copper grids, and stained with uranyl acetate and lead citrate.

BBB Integrity Analysis

For analysis of BBB ultrastructure, microvessels in the motor cortex and striatum of both ipsilateral and contralateral brain hemispheres were examined by an investigator blinded to the animal groups and photographed with an Olympus MegaView III digital camera (ResAlta Research Technologies Corp., Golden, CO.) attached to a FEI Morgagni transmission electron microscope (FEI, Inc., Hillsboro, OR), at 60kV. In addition to the EB extravasation assay described above, vascular EB leakage was analyzed in serial brain sections via immunohistochemistry.

Immunohistochemistry

Immunohistochemical staining for autophagosomes was performed to detect autophagy response within capillary endothelial cells. Serial brain tissue sections of tMCAO and control rats were pre-incubated with 10% normal donkey serum (NGS) and 0.3% Triton 100X in phosphate-buffered saline (PBS) for 60 min at room temperature. Sheep polyclonal anti-Beclin-1 antibody (Beclin-1, 1:200, Thermo Scientific Pierce Antibodies) was applied on the slides overnight at 4°C. The next day, the slides were rinsed in phosphate-buffered saline and incubated with secondary donkey anti-sheep antibody conjugated to FITC (1:500, Alexa Fluor 488, Molecular Probes) for 2 hrs. After rinsing, slides were coverslipped with Vectashield containing DAPI (Vector) and examined using an Olympus BX60 epifluorescence microscope. Observation and quantification of Beclin-1 fluorescent intensity was performed in 5–8 capillaries per examined brain area and structure in both hemispheres: striatum – medial (M), lateral (L), dorsal (D), and ventral (V) areas; motor cortex – M2 and M1 areas. Microvascular EB leakage was also analyzed on these images. Diameters of capillaries (μm) were measured using NIH ImageJ (version 1.46) software. For consistent results, capillaries of diameters from 20–25 μm were used for fluorescent detection of Beclin-1 immunoexpression. Microvessels below or above this range as well as longitude capillaries were excluded.

In a separate set of brain sections, immunohistochemical staining of astrocytes was performed as described (Garbuzova-Davis et al., 2013). Briefly, brain tissues were pre-incubated in blocking solution as described above and then incubated overnight with rabbit polyclonal anti-glial fibrillary acid protein primary antibody (GFAP, 1:500, Dako) at 4°C. The next day, secondary goat anti-rabbit antibody conjugated to FITC (1:500, Invitrogen) was applied for 2 hrs. After washing, slides were coverslipped with Vectashield containing DAPI (Vector) and examined using an Olympus BX60 epifluorescence microscope. Fluorescent images were taken from 2–3 sections per animal separated by approximately 90 μm and analyzed in the same discrete areas of the striatum and motor cortex described above.

Immunohistochemical images of all performed assessments were taken at approximately the same Bregma level analyzed for electron microscopy by an investigator blinded to the experiments and animal codes were removed prior to analysis. To avoid bias in the analysis of fluorescence images, specific brain areas were identified in a section using a 10 \times /0.30 numerical aperture (NA) lens, and then areas of interest were photographed with a 20 \times /0.50 NA lens, photographing the slide in a random raster pattern. All image analyses for Beclin-1

and GFAP were performed by measuring intensity of fluorescent expression ($\%/\mu\text{m}^2$) using NIH ImageJ (version 1.46) software. For Beclin-1 immunoexpression, fluorescent intensity was measured relative to capillary area. For GFAP immunoexpression, fluorescent intensity was measured in the entire image. Thresholds for detection of Beclin-1 and GFAP fluorescein expressions were adjusted for each image to eliminate background noise.

Primary Antibody Characterization

The primary antibodies, their sources, and the dilutions used for immunohistochemistry in this study are listed in Table 1. Immunohistochemical staining for autophagosomes within capillary endothelial cells was performed using a polyclonal sheep anti-Beclin-1 antibody (Cat. No. OSA00006W; 1:200, Thermo Scientific Pierce Antibodies, Rockford, IL, USA). The antigen is a synthetic peptide from amino acid region 400–450 of human Beclin-1 which was conjugated to a blue carrier protein. This region is homologous in rat and mouse and corresponds to a portion of BCL2-interacting protein. This antibody identifies a Beclin-1 protein with Western blotting at approximately 50–55 kDA (manufacturer's technical information; antibody registry No. AB_962043). Immunohistochemical staining of astrocytes was performed using a rabbit polyclonal anti-gial fibrillary acid protein primary antibody (GFAP, Cat No. Z0334; 1:500, Dako, Glostrup, Denmark). This polyclonal antibody was prepared against GFAP from bovine spinal cord. GFAP shows 90–95% homology between species, and as demonstrated by immunocytochemistry, the antibody cross-reacts with GFAP in cat, dog, mouse, rat, and sheep (manufacturer's technical information; antibody registry No. AB_10013382; Fuentes-Santamaria et al., 2013).

Statistical Analysis

Data are presented as means \pm S.E.M. One-way ANOVA with Bonferroni/Dunn's Multiple Comparison test (Statview, Cary, NC, USA) was used. Analyses were considered significant if: EB extravasation – $p < 0.0167$, EB serum concentration – $p < 0.005$, Beclin-1 or GFAP immunoexpression in striatum – $p < 0.0004$, Beclin-1 or GFAP immunoexpression in motor cortex – $p < 0.0018$.

RESULTS

Ultrastructure of the Cerebral Microvasculature in a Chronic Ischemic Rat Model of tMCAO

BBB ultrastructure was analyzed in brains of rats sacrificed at 30 days after tMCAO by electron microscopy. Structural integrity analysis of microvessels in the striatum and motor cortex of the brain was performed on hemispheres ipsilateral and contralateral to tMCAO damage.

Striatum—The striatum in both hemispheres of control rats was characterized by the normal appearance of capillaries surrounded by astrocyte cell processes and myelinated axons (Fig. 1A,B). Capillaries consisted of a single layer of endothelial cells (ECs) surrounded by a basement membrane (BM) layer, sometimes enclosed by additional pericyte cytoplasm. Neurons demonstrated normal morphology with central nuclei (Fig. 1C). Organelles in all cells were well preserved and mitochondria showed a normal pattern of cristae.

In the hemisphere ipsilateral to tMCAO, ultrastructural abnormalities were observed in capillary endothelia in the striatum (Fig. 1D,E). Nearly all ECs showed cytoplasmic formation of autophagosomes, with some autophagosomes extending from lumen to basal lamina in attenuated portions of the cells (Fig. 1D). In several capillaries, large autophagosomes had almost ruptured the lumen of EC membrane. Numerous large vacuoles were seen in EC cytoplasm and perinuclear membrane separation was occasionally observed in EC (Fig. 1E). Pericytes appeared swollen or completely degenerated (Fig. 1D,E). Mitochondria in the cytoplasm of most ECs and pericytes showed disrupted cristae. Near the capillaries were large spaces created by degenerating astrocyte cell processes and protein-filled areas formerly occupied by astrocytes (Fig. 1D). Also, the capillary shown in Figure 1D demonstrated an edematous astrocyte with lipofuscin inclusions. In another striatum capillary (Fig. 1E), two large vacuoles occupied the astrocyte cytoplasm. Figure 1E also shows collagen formation surrounding the capillary, likely due to replacement of degenerated pericyte processes. Myelin sheets in many axons were separated and disrupted (Fig. 1E, black A). Some demyelinated or completely degenerated axons showed evidence of disrupted axoplasmic transport (Fig. 1E, white A). In neuropil of striatum ipsilateral to tMCAO, edematous space between astrocyte, oligodendrocyte, and neuron was noticed (Fig. 1F). Neurons also demonstrated swollen and edematous cytoplasm. Also, uncommon locations of microglia, surrounding or adjacent to capillaries, were detected (data not shown).

In the striatum contralateral to tMCAO insult, considerable vascular damage was observed. Although some capillaries demonstrated normal morphology, numerous capillaries had vacuolated ECs containing large autophagosomes (Fig. 1G). Vacuolization in EC cytoplasm in addition to the perinuclear membrane separation proceeded to almost rupture the EC membrane as shown in one capillary (Fig. 1H). Swollen or degenerated pericytes contained mitochondria with loss of cristae (Fig. 1G). Surrounding the capillaries were degenerated astrocytes showing severe edema and free floating enlarged mitochondria with obvious disruption of the cristae (Fig. 1G,H). Neurons near capillaries displayed swollen (Fig. 1H) or completely degenerated (Fig. 1I) endoplasmic reticulum. In Fig. 1I, dilated nucleus appeared in degenerated neuron, possibly indicating an apoptotic process. Additionally, an entirely degenerated astrocyte containing vacuoles and lipofuscin inclusions was indicated adjacent to this damaged neuron (Fig. 1I).

Motor cortex—Similar to the striatum, motor cortex capillaries in control rats showed normal ultrastructure consisting of microvessels with a single endothelium layer, surrounded by BM and pericyte cytoplasm (Fig. 2A,B). Astrocyte cell processes were adjacent to the outer capillary surface. Myelinated axons were evident and mitochondria showed a normal pattern. Neurons, oligodendrocytes, and astrocytes in close proximity to capillaries demonstrated normal morphology (Fig. 2C).

Thirty days post stroke, in the hemisphere ipsilateral to insult, capillary ultrastructure in motor cortex displayed varied abnormalities (Fig. 2D,E). Edematous ECs with swollen mitochondria were adjacent to healthy ECs in the lumen (Fig. 2D). In numerous motor cortex microvessels, astrocyte cell processes demonstrated dilated endoplasmic reticulum (Fig. 2D) or complete degeneration, as shown by edematous space in their cytoplasm (Fig.

2E). Pericytes also showed a similar profile of dilated endoplasmic reticulum and cytoplasmic lipid drops (Fig. 2E). Axonal myelin degeneration and perivascular edema were noted (Fig. 2E,F). Additionally, a neuron appeared with a swollen nucleus near a capillary and an autophagosome was observed in EC cytoplasm (Fig. 2F).

In the hemisphere contralateral to tMCAO, capillaries in the motor cortex also showed endothelial and pericyte cell damage (Fig. 2G,H). Swollen ECs and autophagosomes in EC cytoplasm were noted in numerous capillaries. Figure 2G showed complete pericyte degeneration with lipofuscin inclusions. In another capillary (Fig. 2H), a swollen pericyte contained enlarged mitochondria with disruption of the cristae. Similarly to the ipsilateral hemisphere, large areas of extracellular edema were observed surrounding the capillary or glial cells (Fig. 2G,H,I). The endothelium thickness was reduced in the area of perivascular edema (Fig. 2H,I). In some motor cortex contralateral areas, edematous spaces were apparent in neurons near their nuclei or in their cytoplasm (Fig. 2I). Interestingly, microglial cells were detected adjacent to capillaries, likely phagocytosing degenerated neural tissue (Fig. 2H).

Thus, BBB alterations were clearly detected by electron microscopy in the striatum and motor cortex of both ipsilateral and contralateral cerebral hemispheres in rats 30 days after tMCAO. Importantly, capillary ultrastructural abnormalities were demonstrated in brain regions remote from the site of primary ischemic injury in chronic phase.

Microvascular Permeability

Capillary BBB permeability was examined via quantitative analysis of Evans Blue extravasation into the brain parenchyma in tMCAO rats and controls. Tissue measurements showed significantly higher EB levels in ipsilateral ($1.45 \pm 0.05 \mu\text{g/g}$, $p < 0.0001$) and contralateral ($1.11 \pm 0.04 \mu\text{g/g}$, $p < 0.0001$) hemispheres vs. controls ($0.68 \pm 0.06 \mu\text{g/g}$) (Fig. 3A). Significantly ($p = 0.0047$) elevated EB level was determined in ipsilateral hemisphere compared to contralateral. These results correlated with our EM findings showing ultrastructural abnormalities in capillary endothelia in striatum and motor cortex microvessels in both ipsilateral and contralateral hemispheres possibly leading to capillary leakage.

Quantification of EB concentrations in sera from tMCAO and control rats was performed as control for cerebral EB extravasation. Expected results showed no significant difference ($p = 0.8127$) in EB concentrations in sera from control ($1.39 \pm 0.06 \mu\text{g/ml}$) vs. tMCAO ($1.42 \pm 0.14 \mu\text{g/ml}$) rats (Fig. 3B) confirming same dye content in stroke and control animals after intravenous injection.

Autophagosomes in Cerebral Endothelial Cells

In view of the fact that our electron microscopy analyses demonstrated ECs containing autophagosomes in numerous striatum and motor cortex capillaries of both ipsi- and contralateral hemispheres 30 days after tMCAO, immunohistochemical analysis of Beclin-1 expression was performed in capillaries from both hemispheres in the striatum (medial (M), lateral (L), dorsal (D), and ventral (V) areas) and motor cortex (M2 and M1 areas). Analyzed capillary diameters in all striatum areas were $23.03 \pm 0.61 \mu\text{m}$ and in M2/M1 motor

cortex – $22.51 \pm 0.52 \mu\text{m}$. Results showed significant ($p < 0.0001$) upregulation of Beclin-1 immunoreexpression in ipsilateral L, D, and V striatum areas of post-stroke rats compared to controls (Fig. 5B; Fig. 4F,G,H). In the contralateral striatum, a significant ($p < 0.0001$) increase of Beclin-1 fluorescent expression was determined in area V (Fig. 5B; Fig. 4I), although elevations of protein expression were seen in M, L, and D areas vs. controls. Importantly, significantly ($p < 0.0001$) higher Beclin-1 immunoreexpression was noted in V striatum (Fig. 4H) compared to area M in ipsilateral hemisphere and M ($p < 0.0001$) and D ($p = 0.0002$) areas of contralateral striatum (Fig. 5B). In the motor cortex, a significant increase of Beclin-1 immunoreexpression in capillary endothelium was determined in M2 ($p = 0.0005$) and M1 ($p < 0.0001$) areas in ipsilateral hemisphere (Fig. 5C, Fig. 4O,P). Overexpression of Beclin-1 in contralateral motor cortex was noted in M2 area (Fig. 4Q). Of note, more extensive Beclin-1 upregulation was shown in ipsilateral M1 capillary ECs ($p = 0.0012$) (Fig. 5C, Fig. 4P) than in M2 or contralateral M1 ($p < 0.0001$) or M2 ($p = 0.0004$) areas. Additionally, immunofluorescence revealed expansion of Beclin-1 in numerous capillaries of analyzed brain structures in both hemispheres (Fig. 4F,H,J,L). Together, our data demonstrated upregulation of Beclin-1 immunoreexpression in capillary endothelium in ipsilateral and contralateral striatum and motor cortex microvessels, likely leading to the endothelium damage and vascular leakage determined by quantitative analysis of EB extravasation. Capillary permeability examined via immunofluorescence expression showed no EB leakage on the abluminal capillary side in the brains of control rats (Fig. 4A–D). At 30 days after tMCAO, EB extravasation was identified at some distance from microvessels in the ipsilateral hemisphere, mostly, in L, D, and V areas of the striatum (Fig. 4F–H) and motor cortex (M1) (Fig. 4P). Extensive EB leakage was also seen in the same areas of cerebral structures in the hemisphere contralateral to initial insult (Fig. 4I–L,Q, R).

Astrocyte Reactivity

Immunohistochemical analysis of astrocytes by GFAP immunoreexpression was performed in the same areas of the striatum and motor cortex in both hemispheres as described for Beclin-1 analysis. In the ipsilateral hemisphere of tMCAO rats, significantly ($p < 0.0001$) elevated GFAP fluorescent expression was determined in all analyzed areas of the striatum (M, L, D, and V) compared to control animals (Fig. 7B, Fig. 6E–H). A significant increase of GFAP immunoreactivity in the contralateral striatum of post-stroke rats vs. controls was demonstrated only in area D ($p = 0.0002$) (Fig. 7B, Fig. 6K). Higher GFAP fluorescent expression was demonstrated in M and D areas of the striatum in post-stroke in ipsilateral hemisphere compared to any analyzed striatal contralateral areas ($p < 0.0001$) (Fig. 7B). There were no statistical differences between tMCAO and control rats in GFAP immunoreexpression within M2 and M1 motor cortex in ipsilateral or contralateral hemisphere (Fig. 7C), although increased GFAP immunoreactivity was shown in ipsilateral M2 area of tMCAO rats (Fig. 6O) vs. controls. Also, ipsilateral M2 motor cortex significantly ($p = 0.0009$) differed from M2 contralateral area in post-stroke animals. Additionally, GFAP positive cells were distinguished surrounding capillaries in the striatum of control brains with detection of EB fluorescence as small red dots attached to the capillary lumen (Fig. 6A–D). In the brains of rats 30 days post-tMCAO, most evidenced astrogliosis in ipsilateral striatum accompanied by microvascular leakage (Fig. 6F,G). Similar capillary leakage was seen in contralateral striatum areas (Fig. 6J–L). Interestingly, EB extravasation in the

striatum and motor cortex of both hemispheres was predominately in capillaries with dissociation of astrocyte end-feet from lumen (Fig. 6F–H,J–L,O–R).

DISCUSSION

Based on our previous study results (Garbuzova-Davis et al., 2013) demonstrating that the damaged BBB plays an important role in subacute diaschisis in the tMCAO ischemic stroke rat model, the present investigation focused on BBB competence in chronic ischemic diaschisis. Although our results showed that most BBB damage (endothelial and pericyte cells impairment, edematous or degenerated perivascular astrocytes, significant EB parenchymal extravasation, endothelial autophagosome accumulation, and increased parenchymal astrocyte reactivity) was detected in the ipsilateral striatum and motor cortex of rats at 30 days after tMCAO, BBB alterations were also identified in the same brain structures of the contralateral hemisphere. Major BBB pathological changes in contralateral remote striatum and motor cortex areas included: (1) vacuolated endothelial cells containing large autophagosomes, (2) degenerated pericytes displaying mitochondria with cristae disruption, (3) degenerated astrocytes and perivascular edema, (4) EB extravasation, and (5) appearance of parenchymal astrogliosis. These pathological alterations were observed not only in the brain regions of primary ischemic injury but also in contralateral cerebral remote areas, suggesting persistent BBB damage in chronic ischemia.

Extensive vascular damage such as BBB impairment in ipsilateral and contralateral cerebral brain structures determined at the ultrastructural level represents a main pathologic feature of chronic tMCAO. Microvascular abnormalities characterized by capillary endothelial and pericyte cell deterioration in addition to perivascular astrocyte degeneration and edema formation in the ipsi- and contralateral hemispheres to MCAO insult strongly evidence compromised BBB integrity at chronic post-stroke condition. Although major ultrastructural BBB damage was observed in the striatum and motor cortex capillaries of the ipsilateral hemisphere, significant but less severe BBB abnormalities were determined in the same brain structures in the hemisphere contralateral to tMCAO at 30 days. This vascular damage in remote brain areas, opposite to the initial stroke insult, might indicate ongoing pathological vascular changes in association with chronic diaschisis.

The pervasive BBB abnormalities evidenced by electron microscopy imaging in both ipsilateral and contralateral hemispheres at 30 days post-tMCAO led to vascular leakage as confirmed by quantitative analysis of Evans Blue extravasation into the brain parenchyma. The extravasated EB level in the ipsilateral and contralateral hemispheres was significantly higher, 2 times and 1.5 times, respectively, compared to non-ischemic controls. Of note, EB extravasation in the contralateral hemisphere was significantly less than in ipsilateral. In comparison with our previous study (Garbuzova-Davis et al., 2013) showing significant EB level in both hemisphere parenchymas in subacute (7 days) tMCAO, half the EB extravasation was noted in chronic (30 days) ischemic tMCAO. Although the reduction in vascular leakage was substantial from subacute to chronic post-stroke stage, significant capillary leakage at 30 days after tMCAO supports previous studies demonstrating BBB leakage for up to 5 weeks (Strbian et al., 2008; Abo-Ramadan et al., 2009). This capillary leakage in the contralateral hemisphere might indicate pervasive BBB damage at chronic

post-stroke stage, leading to the perivascular edema demonstrated by our EM analyses. In both ipsilateral and contralateral hemispheres, the EB extravasation possibly occurs transcellularly or paracellularly due to impaired EC at the structural level as demonstrated in our study or the extravasation may be aided by decreased tight junction integrity under hypoxic condition as shown *in vitro* (Mark and Davis, 2002; Koto et al., 2007) and *ex vivo* (Kago et al., 2006) studies. Also, the elevated EB level in brain parenchyma might result from neovascular permeability. Angiogenesis has been shown to begin shortly after ischemic insult in both rodent models of MCAO and in stroke patients (Marti et al., 2000; Hai et al., 2003; Krupinski et al., 1994) and vessel proliferation continues for up to 3 weeks following experimental cerebral ischemia (Hayashi et al., 2003). Despite the importance of vascular remodeling in neurological post-stroke recovery (Zhang and Chopp, 2009), new cerebral vessels are leaky for several weeks until forming a fully functional BBB (Risau, 1994). Thus, vascular leakage detected by EB extravasation in cerebral hemisphere of initial tMCAO insult and contralateral hemisphere is likely due to compromised endothelial cell integrity and/or neovascular permeability and might contribute to neuronal damage by allowing neurotoxins and other harmful blood-born substances into the CNS. tMCAO rats demonstrated significant motor and neurological dysfunction at 1 month after stroke with substantial neuronal cell losses in the ipsilateral striatum persisting for up to 8 weeks compared to the contralateral hemisphere striatum (Borlongan et al., 1995; Yasuhara et al., 2009). Other reports showed significant correlations between lesion size and histopathological neuronal changes in tMCAO rats for up to 21–60 days post-stroke (Peeling et al., 2001; Sicard et al., 2006). Moreover, a significant decrease of the apical dendritic spine density of the layer V pyramidal neurons in the peri-infarct cortex was determined in the aged mice at 5 months after focal cerebral cortical ischemia (Cui et al., 2013). Although these studies demonstrated neuronal pathological changes predominantly in the brain areas of primary ischemic insult, our ultrastructural analysis revealed numerous neurons with swollen endoplasmic reticulum or edematous cytoplasm and demyelinated axons in the striatum and motor cortex of both ipsilateral and contralateral hemispheres at chronic post-ischemia. Future evaluations focusing on neuronal characteristics in brain areas remote from initial ischemic injury after more prolonged chronic ischemia are needed.

Similar to our previous study (Garbuzova-Davis et al., 2013) showing excessive autophagosome accumulation within capillary endothelium in ipsilateral and contralateral striatum and motor cortex areas in subacute post-tMCAO, the present study also demonstrated a significant increase of autophagosomes in ECs through upregulation of Beclin-1 expression at chronic stage in tMCAO rats. Since autophagy plays an important role in cell survival by degradation of cytosolic components through the autophagosomal-lysosomal pathway (Uchiyama et al., 2008) excessive autophagic processes might induce cellular death (Reggiori and Klionsky, 2002). Increased autophagosomes within neurons in the penumbra were demonstrated at 6 hours post-ischemia in tMCAO (Rami et al., 2008), inducing further neuronal damage after ischemic insult (Sadoshima, 2008; Balduini et al., 2009). Our capillary analyses in specific discrete areas of the striatum and motor cortex in both ipsi- and contralateral hemispheres revealed significant overexpression of Beclin-1 in ECs. Interestingly, immunofluorescent Beclin-1 expression was significantly higher in capillary ECs of the ventral striatum in both ipsilateral and contralateral hemispheres. Since

the ventral striatum is adjacent to the interstitial nucleus of the posterior limb of the anterior commissure (IPAC), an area vital for various afferent brain connections (Alheid et al., 1999; Shammah-Lagnado et al., 1999; Gärtner et al., 2002), it is possible that affected capillaries in this area of both ipsilateral and contralateral hemispheres might negatively influence the amygdala-striatal afferent connections. While the amygdala-striatal transition area has typical striatal connections via cortico- and thalamostriate pathways and is directly or indirectly involved in projections to the substantia nigra (Shammah-Lagnado et al., 1999, 2001; Otake and Nakamura, 2003), the investigation of BBB integrity in these connected remote brain areas from initial ischemic insult might be essential for better understanding post-stroke diaschisis. Another of our findings was significant Beclin-1 overexpression in EC capillaries predominantly of ipsilateral M2 and M1 motor cortex areas with higher expression in M1. Although expression of Beclin-1 in contralateral capillary endothelium of the motor cortex did not significantly differ from controls, elevated marker expression was noted. These capillary endothelium alterations due to autophagosome accumulation, potentially leading to vascular leakage in motor cortex areas, might induce and/or promote neuronal injury in chronic postischemia. Studies have shown extensive neuronal post-ischemic damage in the cerebral cortex, thalamus, brainstem, and spinal cord accompanied by degeneration of corticofugal axonal fibers extending transcallosally into the contralateral hemisphere and caudally along descending tracts indicating remote changes (Iizuka et al., 1989, 1990; Wu and Ling, 1998; Dihné et al., 2002; Ferrer and Planas, 2003; Wang et al., 2012). Moreover, predicting functional potential and recovery in chronic stroke patients depends on corticospinal tract disruption (Stinear et al., 2007; Jayaram et al., 2012). Thus, these results demonstrating upregulation of Beclin-1 expression correlate with our EM observation showing that EC capillaries contained large autophagosomes attenuating portions of the endothelia or even almost rupturing lumen of EC membrane in analyzed brain structures in both hemispheres at 30 days after tMCAO. The extensive autophagosome accumulations within ECs likely led to the BBB dysfunction and vascular leakage determined by quantitative analysis of EB extravasation. The accumulation of autophagosomes in EC likely indicates that these cells have undergone post-ischemic stress, are severely damaged and attempting self-repair. Since many EC are unable to repair themselves through autophagocytosis, they finally die and slough off the capillaries, contributing to the capillary leakage shown in our study. The initial stroke may have switched the EC to an anaerobic metabolism, and they may not have successfully switched back to an aerobic metabolism at chronic post-stroke condition (Wojtkowiak et al., 2012). Possibly the observed EC leakage is due to disruption of normal transport mechanisms and cellular metabolism.

Finally, astrocyte reactivity analyzed in the same specific brain areas in both ipsilateral and contralateral hemispheres used for detection of capillary Beclin-1 expression showed significant increases of GFAP immunoreactivity in all striatal areas of the ipsilateral hemisphere. In the contralateral striatum, significantly elevated GFAP expression was only determined in the dorsal area, although enhanced astrocyte reactivity was noted in remaining regions of the striatum. Yet, it is unclear why bilateral astrocytic overexpression is restricted to only the dorsal striatum. Possibly, astrogliosis in this striatal area reflects spatial differences in astrocyte reactivity due to the striatum's anatomical location proximate to the

corpus callosum. A recent report (Wang et al., 2012) demonstrated degeneration of transcallosal fibers in stroke patients in the subacute or chronic stage using functional MRI. However, this possibility needs further investigation at different post-stroke stages in an animal model. Interestingly, there were no significant differences in GFAP immunoreactivity in M2 and M1 motor cortices between tMCAO and controls in both ipsilateral and contralateral hemispheres. GFAP expression in M2 of ipsilateral hemisphere, however, was significantly higher than M2 on the contralateral side. These results indicate reactive astrogliosis in the ipsilateral striatum in addition to some astrogliosis in remote striatal areas and likely point to chronic post-ischemic inflammation. Since inflammation plays a major role in the pathogenesis of ischemic stroke (del Zoppo and Hallenbeck, 2000; Huang et al., 2006), activated astrocytes (and microglia) might be important contributors to neuroinflammation by secretion of various exacerbating factors such as pro-inflammatory cytokines and chemokines. Although microglial cell response was not directly analyzed in the present study, our ultrastructural examination demonstrated uncommon locations of microglia, surrounding or adjacent to capillaries, in both ipsilateral and contralateral striatum and motor cortices. This observation might indicate migration of microglia to the capillary wall where their activation could induce vascular endothelial inflammation. In an interesting study (Butler et al., 2002), positively double-labeled astrocytes (GFAP) with Fluoro-Jade in the striatum at 21 days after one hour of MCAO in rats demonstrated astrocyte degeneration. Also, the authors described restricted bilateral astrocytic activation in the hippocampus, without contralateral effects in the cortex or striatum, beginning at 1 day and lasting to at least 21 days post-MCAO. Although these study results did not show astrocyte degeneration in the contralateral striatum or cortex after ischemic injury, our EM evaluation provides strong evidence of edematous or entirely degenerated astrocytes not only adjacent to capillaries but also to neurons in the striatum and motor cortex of both ipsilateral and contralateral hemispheres at 30 days tMCAO. Moreover, dissociation of astrocyte end-feet from capillary lumen was demonstrated via immunohistochemistry in analyzed brain structures of both hemispheres. The ultrastructural alterations have been noted in the microvascular BM and BM-astrocyte contacts leading to cerebral edema formation in rats with permanent MCAO (Kwon et al., 2009). These alterations progressed in a time dependent manner during the acute phase of focal ischemia: astrocyte swelling and focal detachment from BM (4 hours), marked astrocyte swelling and decreased contact with BM (8 hours), damaged BM and markedly decreased BM-astrocyte contact (12 hours), BM degradation and ruptured astrocytes (16 hours), excessive water accumulation around microvessels (20 hours), and astrocyte end-feet are no longer visible and BM is faint (48 hours). Since astrocytes mainly regulate cerebral fluid balance via ion and water channels, the astrocyte impairment discussed above which occurs shortly after the ischemic insult is aggravated at subacute (Garbuzova-Davis et al., 2013) and chronic ischemic stages as demonstrated in the present study by significant perivascular edema formation. A comprehensive review (Abbott et al., 2006) emphasized that proper interaction between capillary endothelium and astrocytes within the neurovascular unit is essential for normal BBB maintenance and “investigation of the mechanisms involved in endothelial-astrocytic interaction could help in the design of therapies targeted at specific features necessary for BBB function.” One approach for astrocyte-directed stroke therapy has been discussed (reviewed in (Gleichman and Carmichael, 2013)).

In summary, the compromised BBB integrity detected in chronic post-ischemic rats in cerebral hemisphere capillaries both ipsilateral and contralateral to initial stroke insult might indicate chronic diaschisis. This widespread microvascular damage due to endothelial cell impairment demonstrated by excessive autophagosome accumulation and perivascular astrocyte degeneration could aggravate neuronal deterioration in chronic ischemia. Chronic diaschisis should be considered in the development of treatment strategies for stroke with a primary focus on restoration of endothelial and/or astrocytic integrity towards BBB repair, which might be beneficial for many chronic stroke patients. One potential therapeutic approach for BBB repair in stroke is cell therapy for replacement of damaged endothelial cells by endothelial progenitors. A combination of cellular BBB therapy and inhibition of environmental inflammatory effectors might be a more beneficial treatment strategy for stroke.

Acknowledgments

This study was supported by the NIH (1R01NS071956-01A1) and the James and Esther King Biomedical Research Program (1KG01-33966).

LITERATURE CITED

- Abbott NJ, Rönnbäck L, Hansson E. Astrocyte-endothelial interactions at the blood-brain barrier. *Nat Rev Neurosci.* 2006; 7:41–53. [PubMed: 16371949]
- Alheid GF, Shammah-Lagnado SJ, Beltramino CA. The interstitial nucleus of the posterior limb of the anterior commissure: a novel layer of the central division of extended amygdala. *Ann N Y Acad Sci.* 1999; 877:645–654. [PubMed: 10415676]
- Andrews RJ. Transhemispheric diaschisis. A review and comment. *Stroke J Cereb Circ.* 1991; 22:943–949.
- Anon. Centers for Disease Control and Prevention, National Center for Health Statistics. Compressed Mortality File 1999–2009. CDC WONDER Online Database, compiled for Compressed Mortality File 1999–2009 Series 20, No. 20, 2012. Underlying cause-of-death 1999–2009. 2012. Available from: <http://wonder.cdc.gov/mortSQL.html>
- Ay I, Francis JW, Brown RH Jr. VEGF increases blood-brain barrier permeability to Evans blue dye and tetanus toxin fragment C but not adeno-associated virus in ALS mice. *Brain Res.* 2008; 1234:198–205. [PubMed: 18725212]
- Balduini W, Carloni S, Buonocore G. Autophagy in hypoxia-ischemia induced brain injury: evidence and speculations. *Autophagy.* 2009; 5:221–223. [PubMed: 19029804]
- Belayev L, Busto R, Zhao W, Ginsberg MD. Quantitative evaluation of blood-brain barrier permeability following middle cerebral artery occlusion in rats. *Brain Res.* 1996; 739:88–96. [PubMed: 8955928]
- Borlongan CV, Cahill DW, Sanberg PR. Locomotor and passive avoidance deficits following occlusion of the middle cerebral artery. *Physiol Behav.* 1995; 58:909–917. [PubMed: 8577887]
- Borlongan CV, Hadman M, Sanberg CD, Sanberg PR. Central nervous system entry of peripherally injected umbilical cord blood cells is not required for neuroprotection in stroke. *Stroke J Cereb Circ.* 2004a; 35:2385–2389.
- Borlongan CV, Kaneko Y, Maki M, Yu S-J, Ali M, Allickson JG, Sanberg CD, Kuzmin-Nichols N, Sanberg PR. Menstrual blood cells display stem cell-like phenotypic markers and exert neuroprotection following transplantation in experimental stroke. *Stem Cells Dev.* 2010; 19:439–452. [PubMed: 19860544]
- Borlongan CV, Lind JG, Dillon-Carter O, Yu G, Hadman M, Cheng C, Carroll J, Hess DC. Bone marrow grafts restore cerebral blood flow and blood brain barrier in stroke rats. *Brain Res.* 2004b; 1010:108–116. [PubMed: 15126123]

- Bramlett HM, Dietrich WD. Pathophysiology of cerebral ischemia and brain trauma: similarities and differences. *J Cereb Blood Flow Metab.* 2004; 24:133–150. [PubMed: 14747740]
- Brown RC, Davis TP. Calcium modulation of adherens and tight junction function: a potential mechanism for blood-brain barrier disruption after stroke. *Stroke J Cereb Circ.* 2002; 33:1706–1711.
- Butler TL, Kassed CA, Sanberg PR, Willing AE, Pennypacker KR. Neurodegeneration in the rat hippocampus and striatum after middle cerebral artery occlusion. *Brain Res.* 2002; 929:252–260. [PubMed: 11864631]
- Carmichael ST, Tatsukawa K, Katsman D, Tsuyuguchi N, Kornblum HI. Evolution of diaschisis in a focal stroke model. *Stroke J Cereb Circ.* 2004; 35:758–763.
- Centers for Disease Control and Prevention (CDC). Prevalence and most common causes of disability among adults--United States, 2005. *MMWR Morb Mortal Wkly Rep.* 2009; 58:421–426. [PubMed: 19407734]
- Chen CL, Tang FT, Chen HC, Chung CY, Wong MK. Brain lesion size and location: effects on motor recovery and functional outcome in stroke patients. *Arch Phys Med Rehabil.* 2000; 81:447–452. [PubMed: 10768534]
- Cui L, Murkinati SR, Wang D, Zhang X, Duan W-M, Zhao L-R. Reestablishing neuronal networks in the aged brain by stem cell factor and granulocyte-colony stimulating factor in a mouse model of chronic stroke. *PloS One.* 2013; 8:e64684. [PubMed: 23750212]
- Dankbaar JW, Hom J, Schneider T, Cheng S-C, Bredno J, Lau BC, van der Schaaf IC, Wintermark M. Dynamic perfusion-CT assessment of early changes in blood brain barrier permeability of acute ischaemic stroke patients. *J Neuroradiol.* 2011; 38:161–166. [PubMed: 20950860]
- Dihné M, Grommes C, Lutzenburg M, Witte OW, Block F. Different mechanisms of secondary neuronal damage in thalamic nuclei after focal cerebral ischemia in rats. *Stroke J Cereb Circ.* 2002; 33:3006–3011.
- Dirnagl U, Iadecola C, Moskowitz MA. Pathobiology of ischaemic stroke: an integrated view. *Trends Neurosci.* 1999; 22:391–397. [PubMed: 10441299]
- Dobkin JA, Levine RL, Lagreze HL, Dulli DA, Nickles RJ, Rowe BR. Evidence for transhemispheric diaschisis in unilateral stroke. *Arch Neurol.* 1989; 46:1333–1336. [PubMed: 2590018]
- Ferrer I, Planas AM. Signaling of cell death and cell survival following focal cerebral ischemia: life and death struggle in the penumbra. *J Neuropathol Exp Neurol.* 2003; 62:329–339. [PubMed: 12722825]
- Fuentes-Santamaria V, Alvarado JC, Gabaldon-Ull MC, Manuel Juiz J. Upregulation of insulin-like growth factor and interleukin 1 β occurs in neurons but not in glial cells in the cochlear nucleus following cochlear ablation. *J Comp Neurol.* 2013; 521:3478–3499. [PubMed: 23681983]
- Garbuzova-Davis S, Rodrigues MCO, Hernandez-Ontiveros DG, Tajiri N, Frisina-Deyo A, Boffeli SM, Abraham JV, Pabon M, Wagner A, Ishikawa H, Shinozuka K, Haller E, Sanberg PR, Kaneko Y, Borlongan CV. Blood-brain barrier alterations provide evidence of subacute diaschisis in an ischemic stroke rat model. *PloS One.* 2013; 8:e63553. [PubMed: 23675488]
- Gärtner U, Härtig W, Riedel A, Brauer K, Arendt T. Immunocytochemical evidence for the striatal nature of the rat lateral part of interstitial nucleus of the posterior limb of the anterior commissure (IPAC). *J Chem Neuroanat.* 2002; 24:117–125. [PubMed: 12191728]
- Gleichman AJ, Carmichael ST. Astrocytic therapies for neuronal repair in stroke. *Neurosci Lett* [Internet]. 2013 Available from: <http://dx.doi.org/10.1016/j.neulet.2013.10.055> (<http://www.sciencedirect.com/science/article/pii/S0304394013009592>).
- Go AS, Mozaffarian D, Roger VL, Benjamin EJ, Berry JD, Borden WB, Bravata DM, Dai S, Ford ES, Fox CS, Franco S, Fullerton HJ, Gillespie C, Hailpern SM, Heit JA, Howard VJ, Huffman MD, Kissela BM, Kittner SJ, Lackland DT, Lichtman JH, Lisabeth LD, Magid D, Marcus GM, Marelli A, Matchar DB, McGuire DK, Mohler ER, Moy CS, Mussolino ME, Nichol G, Paynter NP, Schreiner PJ, Sorlie PD, Stein J, Turan TN, Virani SS, Wong ND, Woo D, Turner MB. American Heart Association Statistics Committee and Stroke Statistics Subcommittee. Heart disease and stroke statistics--2013 update: a report from the American Heart Association. *Circulation.* 2013; 127:e6–e245. [PubMed: 23239837]

- Hai J, Li ST, Lin Q, Pan QG, Gao F, King MX. Vascular endothelial growth factor expression and angiogenesis induced by chronic cerebral hypoperfusion in rat brain. *Neurosurg.* 2003; 53:963–972.
- Hayashi T, Noshita N, Sugawara T, Chan PH. Temporal profile of angiogenesis and expression of related genes in the brain after ischemia. *J Cereb Blood Flow Metab.* 2003; 23:166–180. [PubMed: 12571448]
- Huang J, Upadhyay UM, Tamargo RJ. Inflammation in stroke and focal cerebral ischemia. *Surg Neurol.* 2006; 66:232–245. [PubMed: 16935624]
- Iizuka H, Sakatani K, Young W. Corticofugal axonal degeneration in rats after middle cerebral artery occlusion. *Stroke J Cereb Circ.* 1989; 20:1396–1402.
- Iizuka H, Sakatani K, Young W. Neural damage in the rat thalamus after cortical infarcts. *Stroke J Cereb Circ.* 1990; 21:790–794.
- Infeld B, Davis SM, Lichtenstein M, Mitchell PJ, Hopper JL. Crossed cerebellar diaschisis and brain recovery after stroke. *Stroke J Cereb Circ.* 1995; 26:90–95.
- Jayaram G, Stagg CJ, Esser P, Kischka U, Stinear J, Johansen-Berg H. Relationships between functional and structural corticospinal tract integrity and walking post stroke. *Clin Neurophysiol.* 2012; 123:2422–2428. [PubMed: 22717679]
- Jin R, Yang G, Li G. Molecular insights and therapeutic targets for blood-brain barrier disruption in ischemic stroke: critical role of matrix metalloproteinases and tissue-type plasminogen activator. *Neurobiol Dis.* 2010; 38:376–385. [PubMed: 20302940]
- Kago T, Takagi N, Date I, Takenaga Y, Takagi K, Takeo S. Cerebral ischemia enhances tyrosine phosphorylation of occludin in brain capillaries. *Biochem Biophys Res Commun.* 2006; 302:324–329.
- Kahles T, Luedike P, Endres M, Galla H-J, Steinmetz H, Busse R, Neumann-Haefelin T, Brandes RP. NADPH oxidase plays a central role in blood-brain barrier damage in experimental stroke. *Stroke J Cereb Circ.* 2007; 38:3000–3006.
- Kelly-Hayes M, Beiser A, Kase CS, Scaramucci A, D’Agostino RB, Wolf PA. The influence of gender and age on disability following ischemic stroke: the Framingham study. *J Stroke Cerebrovasc Dis.* 2003; 12:119–126. [PubMed: 17903915]
- Koto T, Takubo K, Ishida S, Shinoda H, Inoue M, Tsubota K, Okada Y, Ikeda E. Hypoxia disrupts the barrier function of neural blood vessels through changes in the expression of claudin-5 in endothelial cells. *Am J Pathol.* 2007; 170:1389–1397. [PubMed: 17392177]
- Krupinski J, Kaluza J, Kumar P, Kumar S, Wang JM. Role of angiogenesis in patients with cerebral ischemic stroke. *Stroke.* 1994; 25:1794–1798. [PubMed: 7521076]
- Kuroiwa T, Ting P, Martinez H, Klatzo I. The biphasic opening of the blood-brain barrier to proteins following temporary middle cerebral artery occlusion. *Acta Neuropathol (Berl).* 1985; 68:122–129. [PubMed: 3907257]
- Kwon I, Kim EH, del Zoppo GJ, Heo JH. Ultrastructural and temporal changes of the microvascular basement membrane and astrocyte interface following focal cerebral ischemia. *J Neurosci Res.* 2009; 87:668–676. [PubMed: 18831008]
- Lakhan SE, Kirchgessner A, Tepper D, Leonard A. Matrix metalloproteinases and blood-brain barrier disruption in acute ischemic stroke. *Front Neurol.* 2013; 4:32. [PubMed: 23565108]
- Mark KS, Davis TP. Cerebral microvascular changes in permeability and tight junctions induced by hypoxia-reoxygenation. *Am J Physiol Heart Circ Physiol.* 2002; 282:H1485–H1494. [PubMed: 11893586]
- Marti HJ, Bernaudin M, Bellail A, Schoch H, Euler M, Petit E, Risau W. Hypoxia-induced vascular endothelial growth factor expression precedes neovascularization after cerebral ischemia. *Am J Pathol.* 2000; 156:965–976. [PubMed: 10702412]
- Matsukawa N, Yasuhara T, Hara K, Xu L, Maki M, Yu G, Kaneko Y, Ojika K, Hess DC, Borlongan CV. Therapeutic targets and limits of minocycline neuroprotection in experimental ischemic stroke. *BMC Neurosci.* 2009; 10:126. [PubMed: 19807907]
- Nagasawa H, Kogure K. Correlation between cerebral blood flow and histologic changes in a new rat model of middle cerebral artery occlusion. *Stroke J Cereb Circ.* 1989; 20:1037–1043.

- Neumann-Haefelin T, Witte OW. Periinfarct and remote excitability changes after transient middle cerebral artery occlusion. *J Cereb Blood Flow Metab.* 2000; 20:45–52. [PubMed: 10616792]
- Otake K, Nakamura Y. Forebrain neurons with collateral projections to both the interstitial nucleus of the posterior limb of the anterior commissure and the nucleus of the solitary tract in the rat. *Neuroscience.* 2003; 119:623–628. [PubMed: 12809682]
- Paxinos, G.; Watson, C. *The Rat Brain in Stereotaxic Coordinates (Deluxe Edition)*. Fourth Edition. 4th ed.. Academic Press; 1998.
- Peeling J, Corbett D, Del Bigio MR, Hudzik TJ, Campbell TM, Palmer GC. Rat middle cerebral artery occlusion: correlations between histopathology, T2-weighted magnetic resonance imaging, and behavioral indices. *J Stroke Cerebrovasc Dis.* 2001; 10:166–177. [PubMed: 17903821]
- Persidsky Y, Ramirez SH, Haorah J, Kanmogne GD. Blood-brain barrier: structural components and function under physiologic and pathologic conditions. *J Neuroimmune Pharmacol.* 2006; 1:223–236. [PubMed: 18040800]
- Popp A, Jaenisch N, Witte OW, Frahm C. Identification of ischemic regions in a rat model of stroke. *PLoS One.* 2009; 4:e4764. [PubMed: 19274095]
- Preston E, Sutherland G, Finsten A. Three openings of the blood-brain barrier produced by forebrain ischemia in the rat. *Neurosci Lett.* 1993; 149:75–78. [PubMed: 8469386]
- Abo-Ramadan U, Durukan A, Pitkonen M, Marinkovic I, Tatlisumak E, Pedrono E, Soenne L, Strbian D, Tatlisumak T. Post-ischemic leakiness of the blood-brain barrier: a quantitative and systematic assessment by Patlak plots. *Exp Neurol.* 2009; 219:328–333. [PubMed: 19520075]
- Rami A, Langhagen A, Steiger S. Focal cerebral ischemia induces upregulation of Beclin 1 and autophagy-like cell death. *Neurobiol Dis.* 2008; 29:132–141. [PubMed: 17936001]
- Reggiori F, Klionsky DJ. Autophagy in the eukaryotic cell. *Eukaryot Cell.* 2002; 1:11–21. [PubMed: 12455967]
- Reinecke S, Lutzenburg M, Hagemann G, Bruehl C, Neumann-Haefelin T, Witte OW. Electrophysiological transcortical diaschisis after middle cerebral artery occlusion (MCAO) in rats. *Neurosci Lett.* 1999; 261:85–88. [PubMed: 10081933]
- Risau W. Molecular biology of blood-brain barrier ontogenesis and function. *Acta Neurochir Suppl (Wien).* 1994; 60:109–112. [PubMed: 7526621]
- Rosenberg GA, Estrada EY, Dencoff JE. Matrix metalloproteinases and TIMPs are associated with blood-brain barrier opening after reperfusion in rat brain. *Stroke J Cereb Circ.* 1998; 29:2189–2195.
- Sadoshima J. The role of autophagy during ischemia/reperfusion. *Autophagy.* 2008; 4:402–403. [PubMed: 18367869]
- Sandoval KE, Witt KA. Blood-brain barrier tight junction permeability and ischemic stroke. *Neurobiol Dis.* 2008; 32:200–219. [PubMed: 18790057]
- Seitz RJ, Azari NP, Knorr U, Binkofski F, Herzog H, Freund HJ. The role of diaschisis in stroke recovery. *Stroke J Cereb Circ.* 1999; 30:1844–1850.
- Shammah-Lagnado SJ, Alheid GF, Heimer L. Afferent connections of the interstitial nucleus of the posterior limb of the anterior commissure and adjacent amygdalostriatal transition area in the rat. *Neuroscience.* 1999; 94:1097–1123. [PubMed: 10625051]
- Shammah-Lagnado SJ, Alheid GF, Heimer L. Striatal and central extended amygdala parts of the interstitial nucleus of the posterior limb of the anterior commissure: evidence from tract-tracing techniques in the rat. *J Comp Neurol.* 2001; 439:104–126. [PubMed: 11584811]
- Sicard KM, Henninger N, Fisher M, Duong TQ, Ferris CF. Long-term changes of functional MRI-based brain function, behavioral status, and histopathology after transient focal cerebral ischemia in rats. *Stroke J Cereb Circ.* 2006; 37:2593–2600.
- Stinear CM, Barber PA, Smale PR, Coxon JP, Fleming MK, Byblow WD. Functional potential in chronic stroke patients depends on corticospinal tract integrity. *Brain J Neurol.* 2007; 130:170–180.
- Strbian D, Durukan A, Pitkonen M, Marinkovic I, Tatlisumak E, Pedrono E, Abo-Ramadan U, Tatlisumak T. The blood-brain barrier is continuously open for several weeks following transient focal cerebral ischemia. *Neuroscience.* 2008; 153:175–181. [PubMed: 18367342]

- Tajiri N, Acosta S, Glover LE, Bickford PC, Jacotte Simancas A, Yasuhara T, Date I, Solomita MA, Antonucci I, Stuppia L, Kaneko Y, Borlongan CV. Intravenous grafts of amniotic fluid-derived stem cells induce endogenous cell proliferation and attenuate behavioral deficits in ischemic stroke rats. *PLoS One*. 2012; 7:e43779. [PubMed: 22912905]
- Uchiyama Y, Shibata M, Koike M, Yoshimura K, Sasaki M. Autophagy-physiology and pathophysiology. *Histochem Cell Biol*. 2008; 129:407–420. [PubMed: 18320203]
- VanGilder RL, Huber JD, Rosen CL, Barr TL. The transcriptome of cerebral ischemia. *Brain Res Bull*. 2012; 88:313–319. [PubMed: 22381515]
- Wang LE, Tittgemeyer M, Imperati D, Diekhoff S, Ameli M, Fink GR, Grefkes C. Degeneration of corpus callosum and recovery of motor function after stroke: a multimodal magnetic resonance imaging study. *Hum Brain Mapp*. 2012; 33:2941–2956. [PubMed: 22020952]
- Wojtkowiak JW, Rothberg JM, Kumar V, Schramm KJ, Haller E, Proemsey JB, Lloyd MC, Sloane BF, Gillies RJ. Chronic autophagy is a cellular adaptation to tumor acidic pH microenvironments. *Cancer Res*. 2012; 72:3938–3947. [PubMed: 22719070]
- Wu YP, Ling EA. Transsynaptic changes of neurons and associated microglial reaction in the spinal cord of rats following middle cerebral artery occlusion. *Neurosci Lett*. 1998; 256:41–44. [PubMed: 9832212]
- Yang GY, Betz AL. Reperfusion-induced injury to the blood-brain barrier after middle cerebral artery occlusion in rats. *Stroke J Cereb Circ*. 1994; 25:1658–1664. discussion 1664–1665.
- Yasuhara T, Matsukawa N, Hara K, Maki M, Ali MM, Yu SJ, Bae E, Yu G, Xu L, McGrogan M, Bankiewicz K, Case C, Borlongan CV. Notch-induced rat and human bone marrow stromal cell grafts reduce ischemic cell loss and ameliorate behavioral deficits in chronic stroke animals. *Stem Cells Dev*. 2009; 18:1501–1514. [PubMed: 19301956]
- Zhang ZG, Chopp M. Neurorestorative therapies for stroke: underlying mechanisms and translation to the clinic. *Lancet Neurol*. 2009; 8:491–500. [PubMed: 19375666]
- Del Zoppo GJ, Hallenbeck JM. Advances in the vascular pathophysiology of ischemic stroke. *Thromb Res*. 2000; 98:73–81. [PubMed: 10812160]
- Del Zoppo GJ, Mabuchi T. Cerebral microvessel responses to focal ischemia. *J Cereb Blood Flow Metab*. 2003; 23:879–894. [PubMed: 12902832]

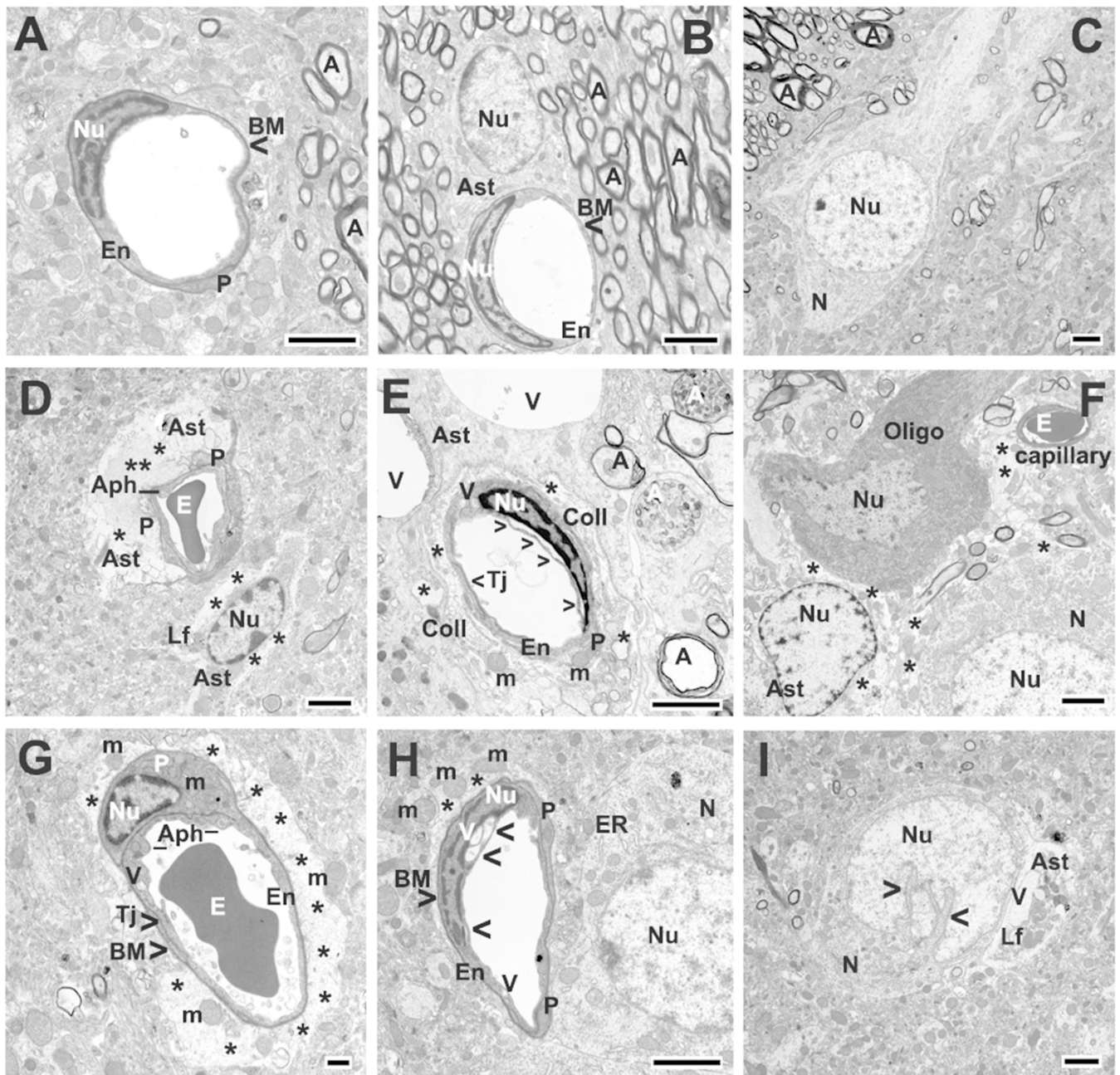


Figure 1.

Electron microscope examination of microvasculature in the rat striatum 30 days after tMCAO. **Control (A–C):** Representative areas of control rat striatum were characterized by the normal ultrastructural appearance of capillaries, motor neurons (N), neuropil, and myelinated axons (A). A single layer of endothelial cells (ECs) was surrounded by a single layer of basement membrane (BM) and enclosed by additional pericyte (P) cytoplasm, forming an intact BBB. Astrocyte (Ast) processes surrounding capillaries showed a normal morphology. **tMCAO 30 days Ipsilateral hemisphere (D–F).** **D:** In the hemisphere ipsilateral to tMCAO insult, ultrastructural abnormalities were observed in striatum capillary

endothelia. ECs showed formation of autophagosomes (Aph) in their cytoplasm, with some autophagosomes extending from lumen to basal lamina in attenuated portions of the cells. Pericytes appeared swollen or completely degenerated. In close proximity to the capillary was a large protein-filled area created by degenerating astrocyte cell processes. Edematous astrocyte with lipofuscin inclusions was noted. **E:** Numerous large vacuoles were seen in EC cytoplasm (arrowheads) and perinuclear membrane separation was occasionally observed in EC. Pericyte was also swollen and contained enlarged mitochondria with disruption of cristae. Two large vacuoles (V) occupy cytoplasm of astrocyte. Collagen (Coll) formation surrounding capillary was detected. Myelin sheets in many axons were separated and disrupted (black A). Two degenerated axons (white A) showed evidence of disrupted axoplasmic transport. **F:** In ipsilateral striatum areas, edematous space between astrocyte, oligodendrocyte (Oligo), and neuron was noticed (*). Neuron also demonstrated swollen and edematous cytoplasm. **tMCAO 30 days Contralateral hemisphere (G–I).** **G:** In contralateral striatum, capillaries contained vacuolated EC with large autophagosomes. A degenerated pericyte occupied by mitochondria (m) with loss of cristae was also apparent. Surrounding the capillary were degenerated astrocytes (*) showing severe edema and free floating enlarged mitochondria. **H:** A capillary with vacuolization in EC cytoplasm in addition to the perinuclear membrane separation (arrowheads) proceeded to almost rupture the cell membrane, was determined. Adjacent to the capillary is an edematous perivascular space (*) containing enlarged mitochondria. Profile of dilated endoplasmic reticulum (ER) was observed in neuron cytoplasm near capillary. **I:** Another neuron with dilated nucleus appeared in contralateral striatum. Entirely degenerated astrocyte containing vacuoles and lipofuscin inclusions (Lf) was observed in close proximity to damaged neuron.

En, endothelial cell; P, pericyte; BM, basement membrane; Ast, astrocyte; E, erythrocyte; Tj, tight junction; m, mitochondrion; A, axon; A (white), disrupted axoplasmic transport; V, vacuole; N, neuron; Nu, nucleus; Aph, autophagosome; ER, swollen endoplasmic reticulum; Lf, lipofuscin inclusion; Coll, collagen; Oligo, oligodendrocyte; arrowheads in E and H indicate separation of luminal EC membrane; arrowheads in I indicate dilated nucleus in neuron. Asterisks in D, E, F, G, and H indicate extracellular edema. Scale bar = 2 μm in A–E and F–I and = 500 nm in G.

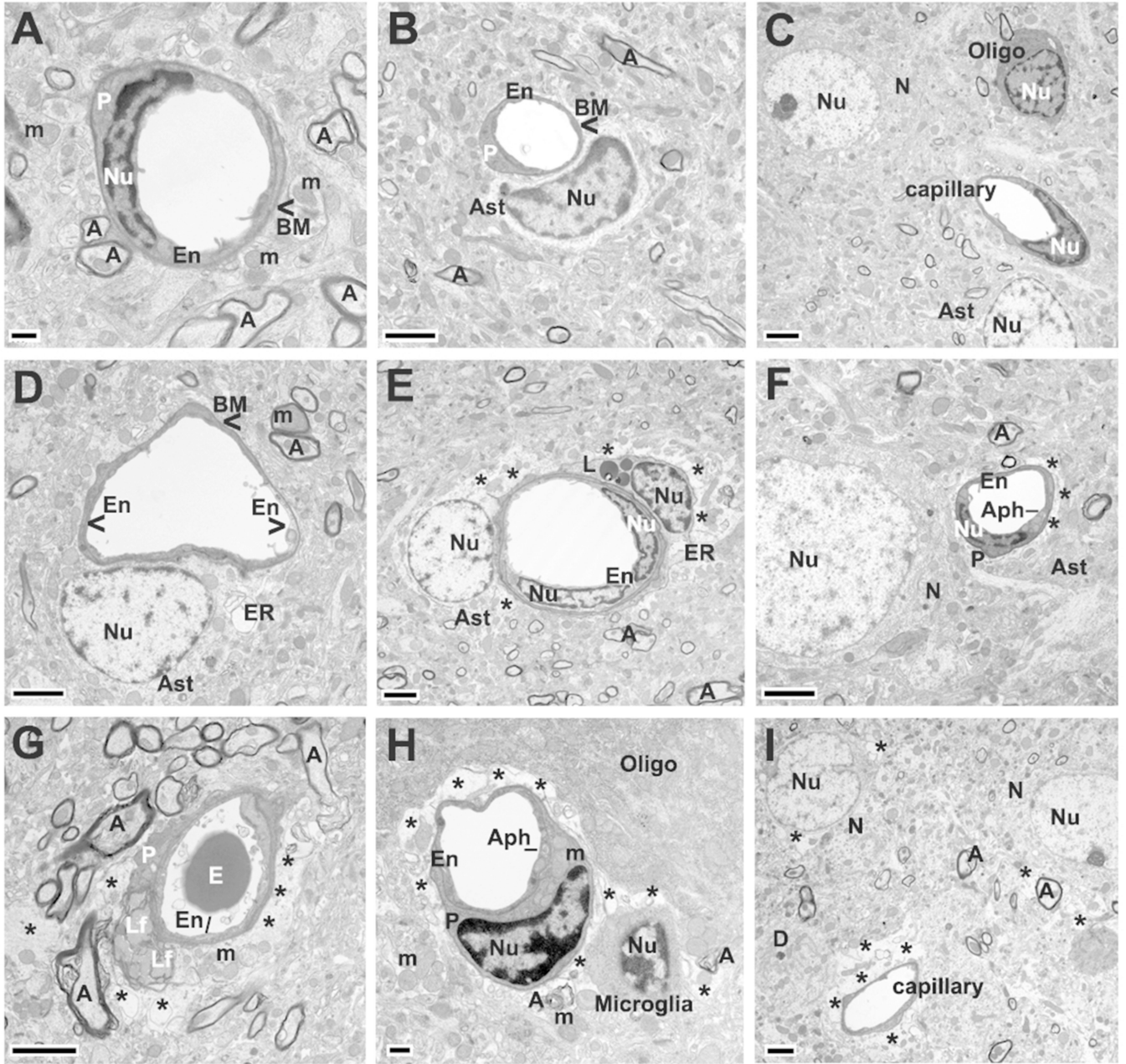


Figure 2. Electron microscope examination of microvasculature in the rat motor cortex 30 days after tMCAO. **Control (A–C).** **A,B:** Similarly to striatum, capillaries in control motor cortex showed normal ultrastructure consisting of microvessels with a single endothelium layer (En), surrounded by BM, and partially bounded by pericyte (P) cytoplasm. Astrocyte (Ast) cell processes were adjacent to the outer capillary surface. Myelinated axons (A) were present and mitochondria showed a normal pattern. **C:** In control motor cortex areas, neurons (N), oligodendrocytes (Oligo), and astrocytes proximal to capillary demonstrated normal morphology. **tMCAO 30 days Ipsilateral hemisphere (D–F).** **D:** In the hemisphere ipsilateral to tMCAO damage, edematous EC with swollen mitochondria were adjacent to

healthy ECs in the lumen. Astrocyte cell processes surrounding capillary demonstrated dilated endoplasmic reticulum (ER). **E:** Completely degenerated astrocyte with edematous cytoplasm was adjacent to capillary. Surrounding the capillary were cell processes of a degenerated pericyte with dilated endoplasmic reticulum and lipid drops (L). **E,F:** There was evidence of extracellular edema and myelin degeneration. **F:** Capillary EC displayed autophagosome (Aph) formation. Neuron appeared with swollen nucleus near capillary.

tMCAO 30 days Contralateral hemisphere (G–I). **G:** In motor cortex of the hemisphere contralateral to tMCAO insult, a capillary was observed with swollen endothelium and complete pericyte degeneration with lipofuscin inclusions. **H:** In another capillary, a swollen pericyte contained enlarged mitochondria (m) with disruption of the cristae in addition to EC containing an autophagosome. Large areas of extracellular edema were observed surrounding the capillary (*). The thickness of endothelium was reduced in the area of perivascular edema. Microglia were detected adjacent to capillary and degenerated myelin. **I:** Edematous spaces (*) were revealed in neurons near nucleus or in their cytoplasm proximal to extracellular edema surrounding capillary.

En, endothelial cell, P, pericyte; BM, basement membrane; Ast, astrocyte; **E**, erythrocyte; m, mitochondrion; A, axon; V, vacuole; N, neuron; Nu, nucleus; Aph, autophagosome; ER, swollen endoplasmic reticulum; L, lipid drop; Lf, lipofuscin inclusion; Oligo, oligodendrocyte; D, dendrite; right arrowhead in d indicates edematous EC with swollen mitochondria. Asterisks in E, F, G, H, and I indicate extracellular edema. Scale bar = 2 μ m in B-G and I and = 500 nm in A, H.

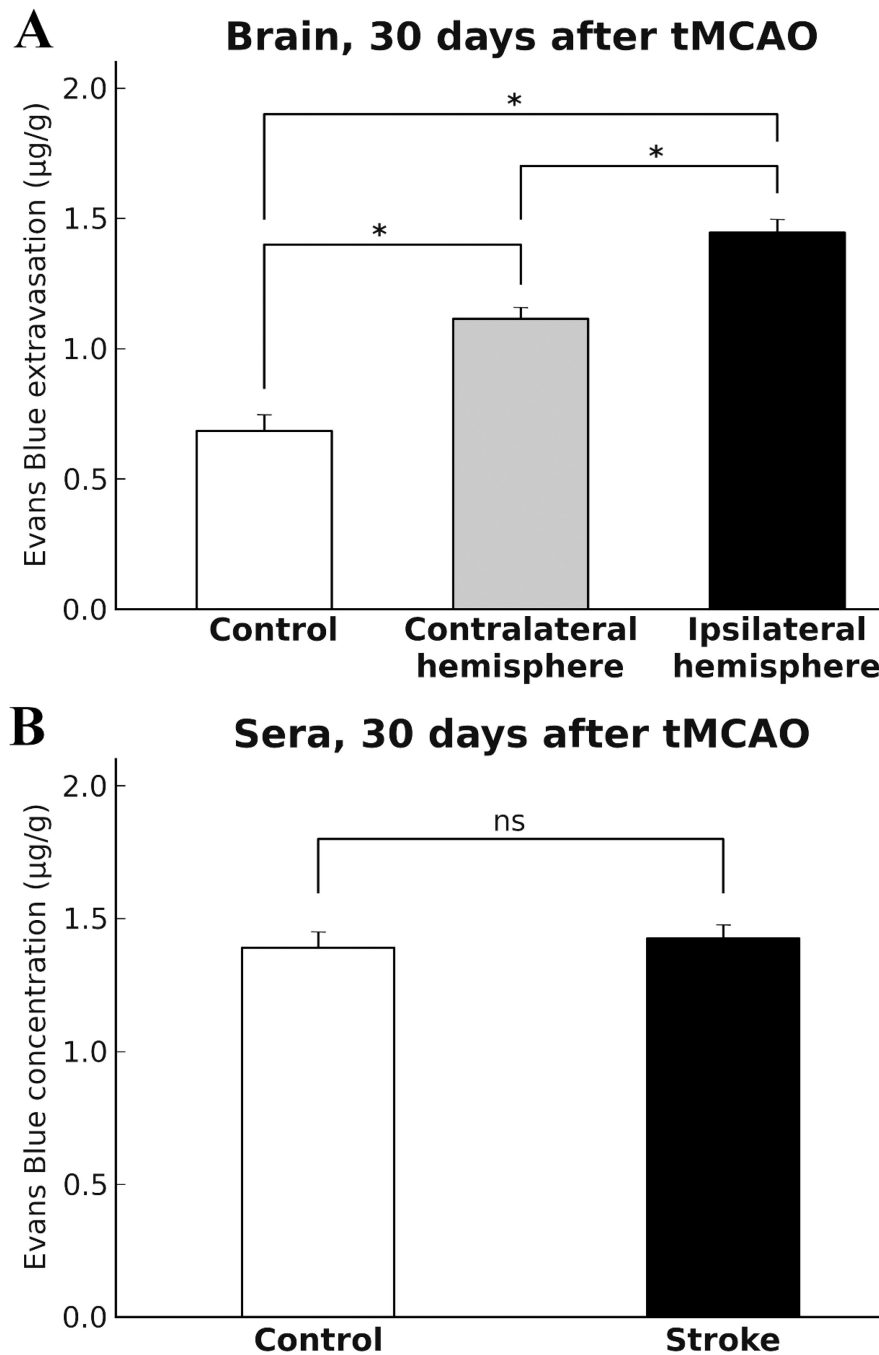


Figure 3. Quantitative analysis of Evans Blue extravasation into the rat brain parenchyma and dye concentration in sera 30 days after tMCAO. **A:** Quantitative measurement of cerebral tissue EB content showed significantly ($p < 0.0001$) higher extravasated EB levels in ipsilateral and contralateral hemispheres vs. control. Significantly ($p = 0.0047$) elevated EB level was determined in ipsilateral hemisphere compared to contralateral. **B:** There was no significant difference in EB concentration in sera from tMCAO rats vs. controls.

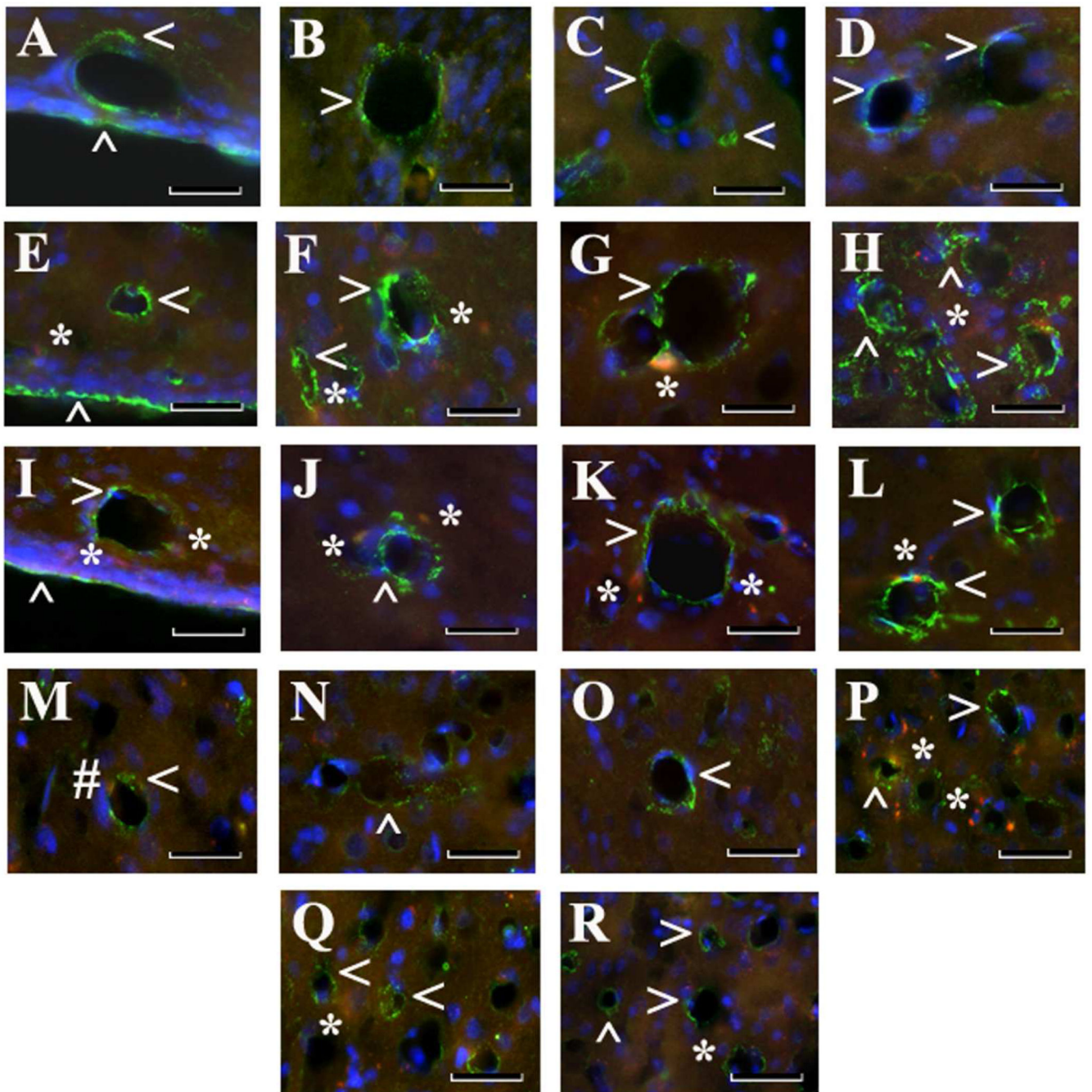


Figure 4.

Immunohistochemical analysis of Beclin-1 immunoreactivity in capillary endothelium in the rat brain 30 days after tMCAO. **Control Striatum Ipsi/Contralateral hemisphere (A–D):** Immunofluorescent staining for Beclin-1 (green, arrowheads) showed typical expression in capillary endothelium of medial (A), lateral (B), dorsal (C), and ventral (D) striatum of control rats. **tMCAO 30 days, Striatum Ipsilateral hemisphere (E–H):** In the ipsilateral hemisphere, extensive Beclin-1 immunoreactivity, indicating autophagosome accumulation within endothelium in numerous striatum capillaries in all analyzed areas, was observed.

tMCAO 30 days, Striatum Contralateral hemisphere (I-L): In the contralateral striatum, higher Beclin-1 expression was determined in lateral (**J**) and ventral (**L**) areas compared to medial (**I**) or dorsal (**K**). In both ipsilateral (**E-H**) and contralateral (**I-L**) striatal capillaries, EB leakage (red, asterisks) was seen. **Motor cortex (M-R):** In motor cortex, increased Beclin-1 immunoeexpression in capillary endothelium was determined in M2 (**O**) and M1 (**P**) areas in ipsilateral hemisphere vs. control (**M,N**). **Q:** Elevated Beclin-1 immunopositivity was noted in M2 contralateral motor cortex. **R:** Beclin-1 immunoeexpression in M1 contralateral motor cortex was slightly elevated compared to M1 control (**N**). EB leakage (red, asterisks) was higher in M1 ipsilateral motor cortex area (**P**). **M:** Of note, EB dye in ipsilateral or contralateral hemispheres of controls was observed within capillary lumen (#). *Striatum:* medial (**A,E,I**), lateral (**B,F,J**), dorsal (**C,G,K**), and ventral (**D,H,L**) areas. *Motor cortex:* control ipsi/contralateral hemisphere (**M** – M2 area, **N** – M1 area), tMCAO 30 days ipsilateral hemisphere (**O** – M2 area, **P** – M1 area), and tMCAO 30 days contralateral hemisphere (**Q** – M2 area, **R** – M1 area). Scale bar = 25 μ m in A-R.

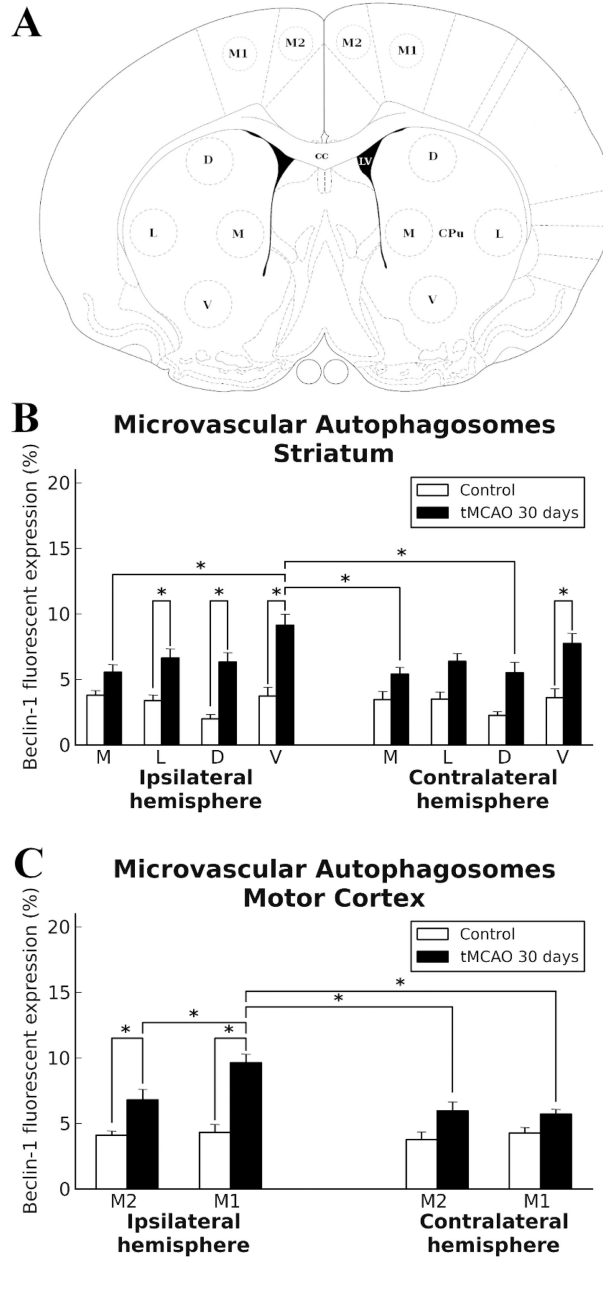


Figure 5. Quantitative analysis of Beclin-1 immunoprecipitation in capillary endothelium in the rat brain 30 days after tMCAO. **A:** Schematic representation of analyzed areas in the striatum and motor cortex in the ipsilateral and contralateral hemispheres. **B:** Significant ($p < 0.0001$) upregulation of Beclin-1 immunoprecipitation was detected in ipsilateral lateral (L), dorsal (D), and ventral (V) striatum areas of post-stroke rats compared to controls. In contralateral striatum, significant ($p < 0.0001$) increase of Beclin-1 fluorescent expression was determined in area V, although elevation of protein expression was demonstrated in medial (M), L, and

D areas vs. controls. **C:** In motor cortex, significant increase of Beclin-1 immunorexpression in capillary endothelium was determined in M2 ($p=0.0005$) and M1 ($p<0.0001$) areas in the ipsilateral hemisphere. Overexpression of Beclin-1 in contralateral motor cortex was noted in M2 area. More extensive Beclin-1 upregulation showed in capillary ECs of ipsilateral M1 ($p=0.0012$) than in M2 and in comparison to contralateral M2 ($p=0.0004$) and M1 ($p<0.0001$) motor cortex areas.

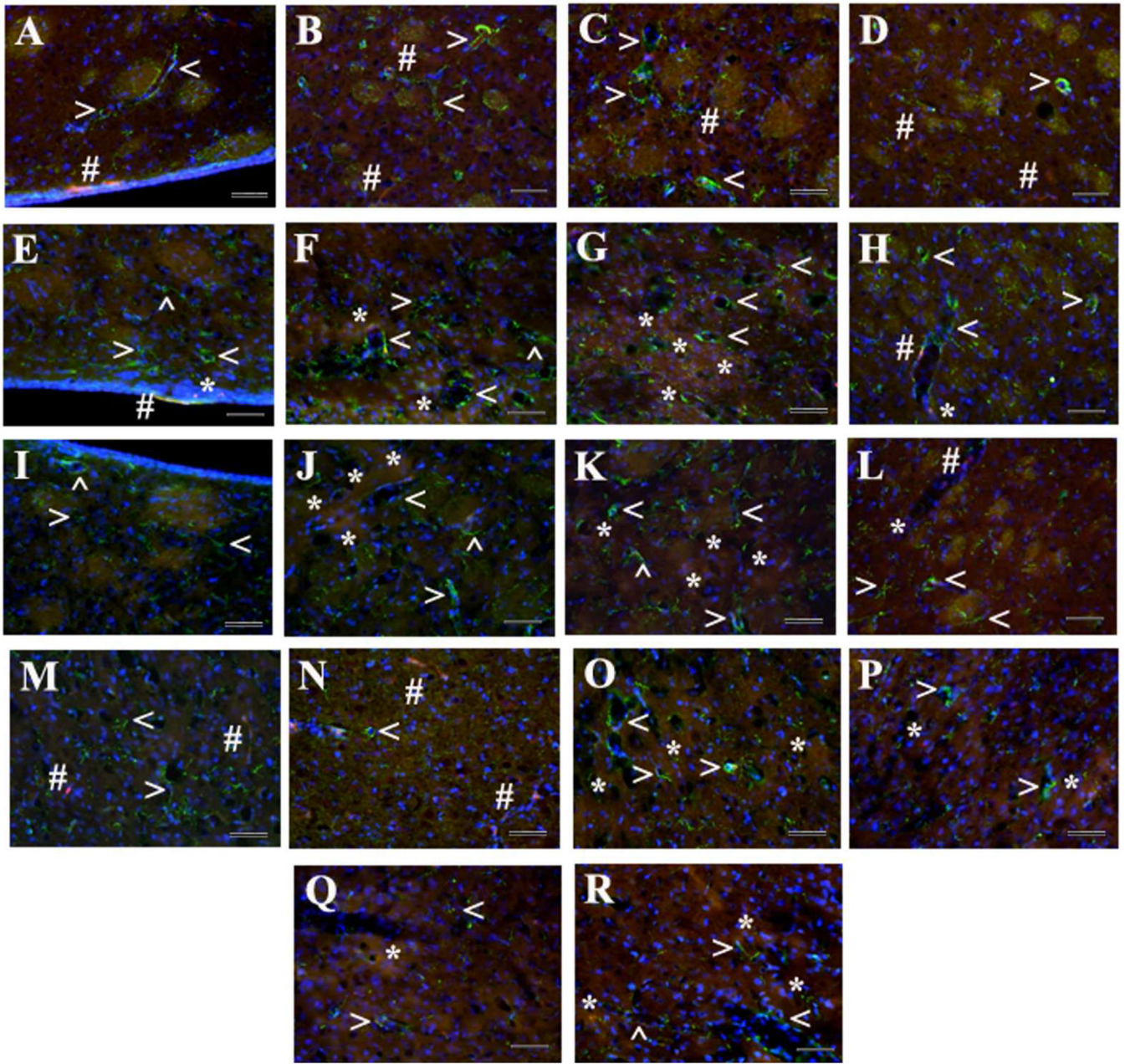


Figure 6. Immunohistochemical analysis of GFAP immunoreactivity in the rat brain 30 days after tMCAO. **Control Striatum Ipsi/Contralateral hemisphere (A–D):** Normal appearance of parenchymal GFAP positive cells with well-defined astrocytes surrounding capillaries (green, arrowheads) was seen in all examined striatal areas of ipsilateral or contralateral hemisphere in control rats. EB dye was visible as small red dots (#) attached to the capillary lumen. **tMCAO 30 days, Striatum Ipsilateral hemisphere (E–H):** In the ipsilateral hemisphere of tMCAO rats, increased GFAP immunoreactivity, indicating astroglia, was determined in all analyzed striatal areas. **tMCAO 30 days, Striatum Contralateral hemisphere (I–L):** Similar, but less intensive, GFAP immunoreactivity was observed in

contralateral striatum. EB capillary leakage was mostly detected in lateral and dorsal areas of ipsilateral (**F,G**, red, asterisks) and contralateral (**J,K**, red, asterisks) striatum. **Motor cortex (M–R)**: In motor cortex, GFAP immunoreexpression in M2 and M1 areas in ipsilateral (**O,P**) and contralateral (**Q,R**) hemispheres of tMCAO rats did not differ from controls (**M,N**). Importantly, dissociation of astrocytes from capillary lumen was observed in the striatum (**F–H,J–L**) and motor cortex (**O–R**) of both hemispheres in tMCAO rats. *Striatum*: medial (**A,E,I**), lateral (**B,F,J**), dorsal (**C,G,K**), and ventral (**D,H,L**) areas. *Motor cortex*: control ipsi/contralateral hemisphere (**M** – M2 area, **N** – M1 area), tMCAO 30 days ipsilateral hemisphere (**O** – M2 area, **P** – M1 area), and tMCAO 30 days contralateral hemisphere (**Q** – M2 area, **R** – M1 area). Scale bar = 50 μ m in A–R.

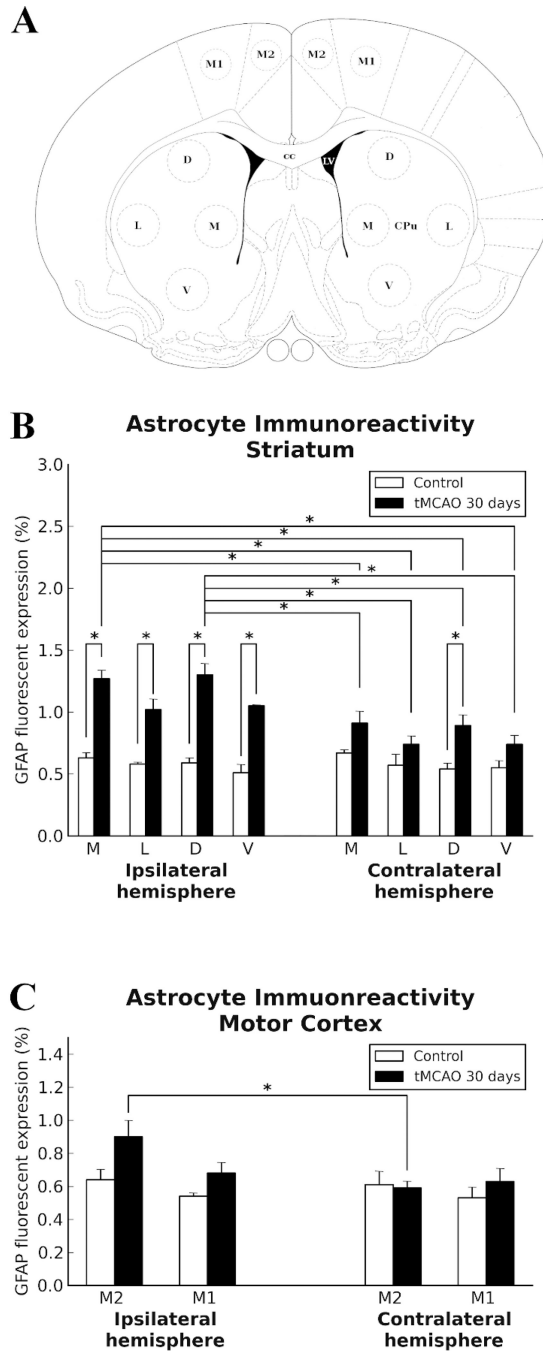


Figure 7. Quantitative analysis of GFAP immunoreactivity in the rat brain 30 days after tMCAO. **A:** Schematic representation of analyzed areas in the striatum and motor cortex in the ipsilateral and contralateral hemispheres. **B:** In ipsilateral striatum of tMCAO rats, significantly ($p < 0.0001$) elevated GFAP immunoreactivity was determined in all analyzed areas (M, L, D, and V) vs. controls. Only significant ($p = 0.0002$) increase of GFAP immunoreactivity was determined in area D of contralateral striatum. **C:** There were no significant differences between tMCAO and control rats in GFAP immunoreactivity in M2 and M1 motor cortices

in ipsilateral or contralateral hemisphere, although elevation of GFAP immunoexpression was determined in ipsilateral M2 area of tMCAO rats. Also, ipsilateral M2 area of motor cortex was significantly ($p=0.0009$) higher than in contralateral side in tMCAO rats.

Table 1

Primary Antibodies Used

Antigen	Immunogen	Manufacturer	Catalog/lot number/species	Dilution used
Beclin-1	Synthetic peptide from human coiled-coil myosin-like BCL2-interacting protein	Thermo Scientific Pierce Antibodies (Rockford, IL)	OSA00006W/0D 1691051/ Sheep polyclonal	1:200
GFAP	Polyclonal rabbit anti-gial fibrillary acidic protein. GFAP isolated from cow spinal cord	Dako (Glostrup, Denmark)	Z0334/00073720/ Rabbit polyclonal	1:500